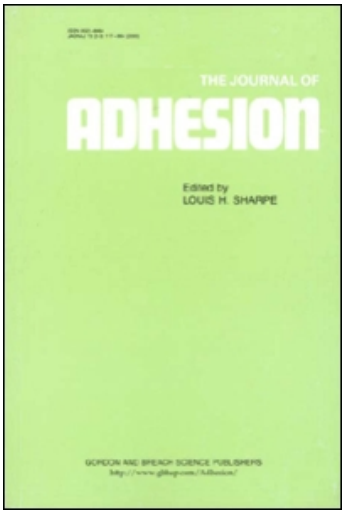

The Journal of Adhesion
Publication details, including instructions for authors and subscription information:
http://www.informaworld.com/smpp/title~content=t713453635

The influence of adhesive bondline thickness imperfections on stresses in composite joints

Hyonny Kim[a]
[a] School of Aeronautics and Astronautics, Purdue University, West Lafayette, Indiana, USA

Online publication date: 08 September 2010

To cite this Article Kim, Hyonny(2003) 'The influence of adhesive bondline thickness imperfections on stresses in composite joints', The Journal of Adhesion, 79: 7, 621 — 642
To link to this Article: DOI: 10.1080/00218460309578
URL: http://dx.doi.org/10.1080/00218460309578

The Journal of Adhesion, 79: 621–642, 2003

ISSN: 0021-8464
DOI: 10.1080/00218460390219528

Taylor & Francis
Taylor & Francis Group

THE INFLUENCE OF ADHESIVE BONDLINE THICKNESS IMPERFECTIONS ON STRESSES IN COMPOSITE JOINTS

Hyonny Kim
School of Aeronautics and Astronautics, Purdue University,
West Lafayette, Indiana, USA

Adhesively-bonded joints can have spatial variations in bondline thickness with respect to their overlap length. Assumptions pertaining to shear-lag and adherend transverse shear deformation are used to compose a governing differential equation that permits any mathematical function to be used for representing the variation in bondline thickness, $t_a(x)$. Finite Difference solution techniques are employed to solve this equation, and it is shown by a series of case study example calculations that the adhesive shear stress changes significantly for deviations about a baseline, uniform thickness, configuration. It is also shown that for cases when the gradient in bondline thickness is small, simple closed-form solutions developed strictly for uniform thickness joints can provide reasonable accuracy. Numerical results are summarized as "stress concentration factor" curves, allowing quick estimation of the upper and lower bounds of normalized peak shear stress in joints having varying degrees of thickness imperfection.

Keywords: Stress analysis; Varying bondline; Thickness defect; Composite bonding; Joint design

INTRODUCTION

An analysis is presented that predicts the shear stress in an adhesively bonded composite joint having continuously varying bondline

Received 21 September 2002; in final form 3 December 2002.

This article is dedicated to the late Don Oplinger who passed away on June 12, 2000. His personal interest in this topic of stresses in varying bondline thickness motivated the theoretical developments reported herein. Dr. Larry Ilcewicz and Dr. Peter Shyprykevich of the Federal Aviation Administration are acknowledged for their technical interest. Financial support of this research was provided under FAA Cooperative Agreement No. 01-C-AW-UCSB.

Address correspondence to Hyonny Kim, School of Aeronautics and Astronautics, Purdue University, 315 N. Grant Street, West Lafayette, IN 47907-2023, USA. E-mail: hyonny@ecn.purdue.edu

thickness. Varying bondline thickness can occur during the manufacture of joints, particularly for thin adherends that are relatively flexible in bending, and in cases when blind assembly is involved. In most cases, the source of this problem is due to difficulties that can be encountered in applying proper fixturing to the parts during adhesive cure. A common scenario is one where the bondline thins at one or both ends of the overlap, *i.e.*, it "pinches off." An example of pinch-off is shown in Figure 1. This pinch-off at the ends of the bond overlap is particularly undesirable since the thinner adhesive layer results in higher adhesive shear stress exactly in the location where the highest shear stress already exists.

It is desirable to have an analytical procedure to predict the effect of thickness variation on the shear stress in the adhesive. Such an analysis is useful, particularly for design engineers, when evaluating the effects of bond thickness control (*e.g.*, during manufacture) on joint performance. Classical analyses, based on shear-lag, have been developed to predict the adhesive shear stress in joints of uniform bond thickness [1, 2]. Improvements to the classical theory include accounting for plasticity in the adhesive prior to failure [3], predicting peel stress in single-lap joints [4–6], and allowing for transverse (through-the-thickness) shear deformation of the adherends [7]. This latter improvement is an important factor to include in the analysis of bonded polymer matrix composites since the transverse shear modulus of these materials, relative to the in-plane Young's modulus, is generally much smaller than for isotropic materials.

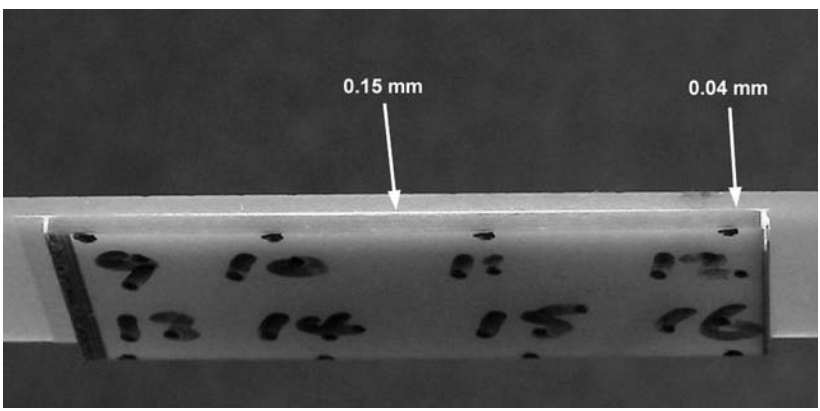

FIGURE 1 Pinch-off in glass/epoxy adherends bonded with FM 73 adhesive. Adherend thickness is 0.89 mm. Adhesive thickness varies from 0.04 mm at ends to 0.15 mm at center of bondline.

To the author's best knowledge, there are no theoretical works that rigorously accommodate a varying bondline thickness during their derivation. Hart-Smith [3] includes a discussion of pinch-off and flaring (which is the opposite of pinch-off) at a qualitative level. Most studies investigating the effect of bondline thickness are limited to joints of uniform thickness [5, 8–11]. Gleich *et al*. [8] and Li *et al*. [9] have shown by numerical analyses that the shear and peel stresses are not uniform through the adhesive thickness, particularly at the ends of the joint overlap. To address this thickness-wise variation, Kline [10] presented a general joint analysis theory that predicts adhesive shear and peel stresses by assuming a linear variation of these stresses through the adhesive. Additionally, Wang and Rose [11] present compact solutions to predict the complex stress distribution, including the singularity stresses existing at the ends of a joint. Joints having thickness variation have been analyzed numerically by Rispler *et al*. [12]. This work focused on internally tapered adherends which result in gradually larger adhesive thickness at the overlap ends.

The focus of this article is the prediction of shear stress in the adhesive due to continuously varying bondline thickness in the overlap length direction of the joint. While this analysis is based on shear lag assumptions and therefore only predicts adhesive shear stress, it can be considered as a nominal solution on top of which refinements, or corrective solutions, can be added.

THEORY

The analysis presented in this paper is restricted to cases where the joint is either in a symmetric double-lap configuration, or the adherends are supported so that out-of-plane bending is restricted. As the formulation is based on shear-lag theory, only shear stress in the adhesive is predicted, and not peel stress. A modified version of the transverse shear deformation correction introduced by Tsai *et al*. [7] has been incorporated in the present theoretical development, and the general procedure by which transverse shear flexibility is accounted for is credited to these authors.

Notation that is used to describe the joint is indicated in Figure 2. The upper adherend shown in the figure will be referred to as the outer adherend, whereas the lower is referred to as the inner since, in the double-lap configuration, this adherend would be surrounded on both sides by outer adherends.

A second-order differential equation with nonconstant coefficients is to be derived that describes the transfer of load from one adherend to the next. The derivation of this equation assumes the following:

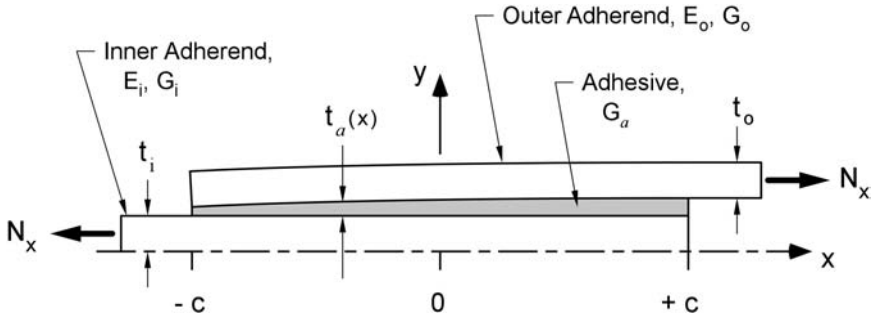

FIGURE 2 Varying bondline thickness joint geometry for double-lap or supported single-lap joint.

1. symmetric double-lap or supported single-lap joint configuration,
2. adherends have constant thickness,
3. uniform shear strain profile through the adhesive thickness,
4. adhesive carries only out-of-plane shear stresses,
5. linear elastic material behavior, and
6. small angles resulting from bondline thickness variation.

The in-plane displacement profile in each adherend, $u_o(y_o)$ and $u_i(y_i)$, are shown in Figure 3. Note that these profiles account for transverse shear flexibility and, therefore, the displacements at the adherend-to-adhesive interfaces, u_{oa} and u_{ia}, are not necessarily the same as the corresponding displacements at the outer adherend free surface, u_{os}, and inner adherend center (or free surface for supported single-lap case), u_{ic}. For adherends with no shear flexibility, there will be uniform displacement through the adherend thickness, as indicated by the dashed-line profile in Figure 3.

In a modification to the treatment by Tsai *et al*. [7], the assumption is made that the transverse shear stress varies quadratically through the thickness of the adherends, as is shown in Figure 3. Note as per assumption 6 above, that the thickness of the adherends, along the y_o and y_i axes directions, are t_o and t_i. This assumed profile will be used to express the in-plane stress resultants, T_o and T_i, carried by the outer and inner adherends, respectively. The transverse shear stresses τ_o and τ_i in the outer and inner adherends are

$$\tau_o = \tau_a \left(1 - \frac{2y_o}{t_o} + \frac{y_o^2}{t_o^2} \right) \tag{1}$$

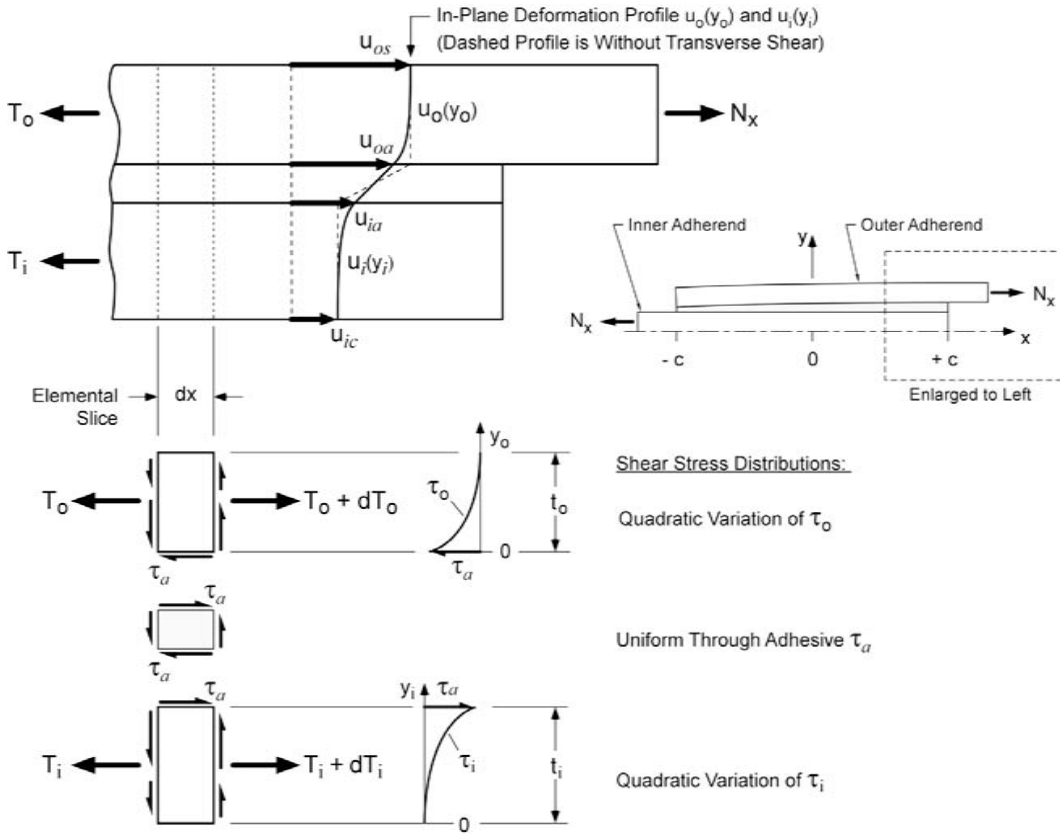

FIGURE 3 Adherend deformation and quadratic variation of transverse shear stress.

and

$$\tau_i = \tau_a \frac{y_i^2}{t_i^2}. \tag{2}$$

In Equations (1) and (2), τ_a is the shear stress in the adhesive, and it is assumed that τ_a is uniform through the thickness of the adhesive as per assumption 3. t_o and t_i are the thickness of the outer and inner adherends, respectively. y_o and y_i are local coordinate systems as defined in Figure 3.

The shear strains in the outer and inner adherends can be expressed as

$$\gamma_o = \frac{du_o}{dy_o} = \frac{\tau_o}{G_o} \tag{3}$$

and

$$\gamma_i = \frac{du_i}{dy_i} = \frac{\tau_i}{G_i}, \tag{4}$$

where G_o and G_i are the transverse (interlaminar) shear moduli of the adherends. Integrating Equation (3) from 0 to y_o and recognizing that at $y_o = 0$, $u_o = u_{oa}$, the in-plane displacement in the outer adherend is determined:

$$u_o(y_o) = \frac{\tau_a}{G_o}\left(y_o - \frac{y_o^2}{t_o} + \frac{y_o^3}{3t_o^2}\right) + u_{oa}. \tag{5}$$

Similarly, integrating Equation (4), with $u_i = u_{ia}$ at $y_i = t_i$, the in-plane displacement in the inner adherend is

$$u_i(y_i) = \frac{\tau_a}{2G_i t_i}\left(\frac{y_i^3}{t_i^2} - t_i\right) + u_{ia}. \tag{6}$$

The stress resultants carried by the outer and inner adherends can now be calculated.

$$T_o = \int_0^{t_o} \sigma_o dy_o = \int_0^{t_o} E_o \frac{du_o}{dx} dy_o = E_o t_o \left(\frac{du_{oa}}{dx} + \frac{d\tau_a}{dx} \cdot \frac{t_o}{4G_o}\right), \tag{7}$$

$$T_i = \int_0^{t_i} \sigma_i dy_i = \int_0^{t_i} E_i \frac{du_i}{dx} dy_i = E_i t_i \left(\frac{du_{ia}}{dx} - \frac{d\tau_a}{dx} \cdot \frac{t_i}{4G_i}\right), \tag{8}$$

where σ_o and σ_i are the in-plane longitudinal stresses, and E_o and E_i are the Young's moduli for the outer and inner adherends, respectively.

A relationship between the adhesive shear stress τ_a and the load in the outer adherend T_o can be written by performing a force balance on the elemental slice of outer adherend shown in Figure 3:

$$\tau_a = \frac{dT_o}{dx}. \tag{9}$$

Another relationship important to this derivation is the global force balance through the entire joint at any position along the lap length,

$$T_o + T_i = N_x. \tag{10}$$

In Equation (10), N_x is the applied load (in units of force per unit length). The shear stress in the adhesive is defined as

$$\tau_a = \frac{G_a}{t_a(x)}(u_{oa} - u_{ia}), \tag{11}$$

where G_a is the shear modulus of the adhesive, and $t_a(x)$ is the x-dependent adhesive thickness. Taking the first derivative of Equation (11) with respect to x results in

$$\frac{dt_a}{dx}\tau_a + t_a\frac{d\tau_a}{dx} = G_a\left(\frac{du_{oa}}{dx} - \frac{du_{ia}}{dx}\right). \tag{12}$$

Combining Equation (12) with Equations (7) through (10) results in a second-order differential equation governing the load carried by the outer adherend:

$$\frac{d^2T_o}{dx^2} + \frac{1}{t_a\alpha^2}\cdot\frac{dt_a}{dx}\cdot\frac{dT_o}{dx} - \frac{\lambda^2}{\alpha^2}T_o + \frac{C_o}{\alpha^2} = 0, \tag{13}$$

with grouped terms λ^2, α^2, and C_o defined as

$$\lambda^2 = \frac{G_a}{t_a}\left(\frac{1}{E_it_i} + \frac{1}{E_ot_o}\right) \tag{14}$$

$$\alpha^2 = 1 + \frac{G_a}{t_a}\left(\frac{t_i}{4G_i} + \frac{t_o}{4G_o}\right) \tag{15}$$

$$C_o = \frac{G_aN_x}{t_at_iE_i} \tag{16}$$

Note that the coefficients of Equation (13) contain the varying bondline thickness $t_a(x)$. In general, t_a can be any arbitrary function in x representing the bondline thickness. Solution of the governing equation, subject to the boundary conditions

$$T_o(-c) = 0 \tag{17}$$

and

$$T_o(+c) = N_x, \tag{18}$$

determines the in-plane stress resultant T_o in the outer adherend. The shear stress in the adhesive can then be calculated using Equation (9).

SOLUTION

For the case of t_a being uniform, the coefficients of Equation (13) become constant, and the term containing first derivatives of t_a and T_o becomes zero. The closed-form solution to the governing equation is then

$$T_o = A_o \cosh(\tfrac{\lambda}{\alpha}x) + B_o \sinh(\tfrac{\lambda}{\alpha}x) + \frac{C_o}{\lambda^2}. \tag{19}$$

The constants A_o and B_o are determined using the two boundary conditions on the outer adherend, Equations (17) and (18). Using Equation (9), the solution for shear stress in the adhesive is

$$(\tau_a)_{UBT} = \frac{\lambda}{\alpha}\left[\left(\frac{N_x}{2} - \frac{C_o}{\lambda^2}\right)\frac{\sinh(\frac{\lambda}{\alpha}x)}{\cosh(\frac{\lambda}{\alpha}c)} + \frac{N_x}{2}\cdot\frac{\cosh(\frac{\lambda}{\alpha}x)}{\sinh(\frac{\lambda}{\alpha}c)}\right]. \tag{20}$$

This result is given the subscript UBT to denote a solution for a joint with uniform bondline thickness (UBT) and therefore constant coefficients in the governing Equation (13). To remove the effects of adherend transverse shear flexibility from this solution, G_o and G_i can be set to infinity, causing $\alpha = 1$. The resulting shear stress can be expressed as

$$(\tau_a)_{\text{Volkersen}} = \lambda\left[\left(\frac{N_x}{2} - \frac{C_o}{\lambda^2}\right)\frac{\sinh(\lambda x)}{\cosh(\lambda c)} + \frac{N_x}{2}\cdot\frac{\cosh(\lambda x)}{\sinh(\lambda c)}\right]. \tag{21}$$

This result is given the subscript *Volkersen* [1] to denote that Equation (21) is the classical solution attributed to that author.

It is possible to use Equations (20) and (21) to compute shear stress in a joint by simply substituting in a varying bondline thickness function, $t_a(x)$. However, note that these solutions are not rigorously applicable to cases of varying bondline thickness since they have been derived based on the assumption of uniform thickness. Solution of Equation (13) for the case of arbitrarily-varying bond thickness can be accomplished by using a Finite Difference numerical method. To use this method, the outer adherend is discretized into n equally sized regions of length $\Delta x = 2c/n$, as shown in Figure 4. The governing equation is represented by approximations to the derivative terms

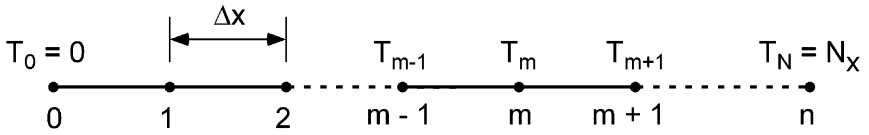

FIGURE 4 Finite difference discretization of outer adherend.

contained in the equation. Solution for the value T_m at node m is then possible using the following difference equation:

$$T_m = \frac{\frac{T_{m+1}+T_{m-1}}{\Delta x^2} + \frac{1}{\alpha^2 t_a} \cdot \frac{\left(t_a^{m+1} - t_a^{m-1}\right)\left(T_{m+1} - T_{m-1}\right)}{4\Delta x^2} + \frac{C_o}{\alpha^2}}{\frac{2}{\Delta x^2} + \frac{\lambda^2}{\alpha^2}}. \tag{22}$$

Equation (22) can be programmed into a digital computer using any popular programming language, mathematical software, or even a spreadsheet program. The boundary conditions, Equations (17) and (18), are assigned to the end nodes, as shown in Figure 4, and a converged solution is generated after many iterations (typically on the order of 10^3). The numerical x-derivative of the solution represented by Equation (22) is the adhesive shear stress and will be referred to as the Variable Bondline Thickness (VBT) solution. Since this is a numerical solution, convergence of the results is an important consideration. A convergence study is discussed in more detail in a later section of this paper.

EXAMPLE CALCULATIONS

The VBT solution to Equation (13) is demonstrated using several example calculations. For each example, the VBT prediction is compared with the UBT solution given by Equation (20), the Volkersen [1] solution given by Equation (21), and with Finite Element Analysis (FEA) results. The VBT Finite Difference results were produced for a node spacing of $\Delta x = 0.127$ mm. The linear static FEA results were obtained using 8-noded plane strain elements CPE8R in the commercial software ABAQUS [13]. In all FEA models, a minimum element dimension of 0.0063 mm was used to represent the adhesive at $x = -c$. A typical mesh shown in Figure 5 illustrates the degree of refinement needed at these critical locations in order to accurately predict stresses in the adhesive. Boundary conditions were applied such that the mesh in Figure 5 represents half of a symmetric double lap, or supported single lap joint: constraint in the y- and x-directions along the bottom and lefthand edges, respectively, and a uniform pressure applied to the righthand edge.

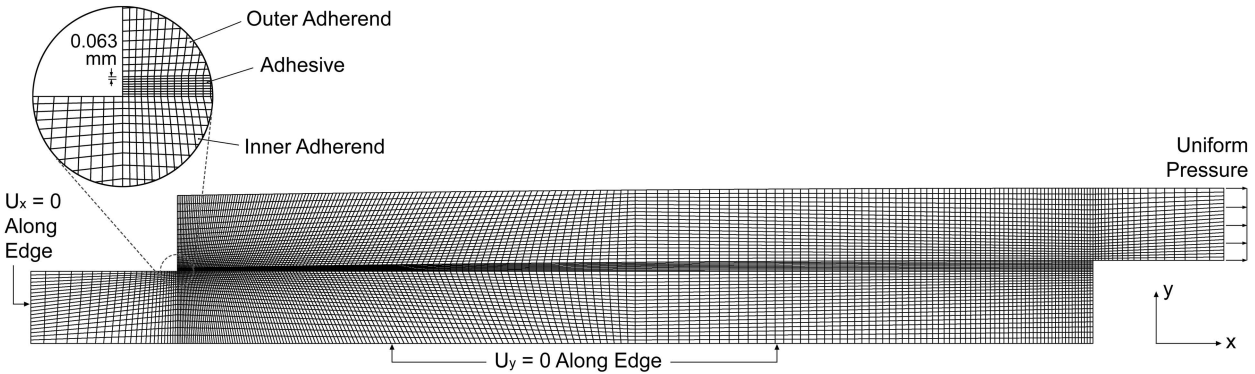

FIGURE 5 FEA mesh for joint with 0.051 to 0.152 mm bondline thickness variation.

TABLE 1 Joint Parameters for Example Calculations

Parameter	Value
Adherends—quasi-isotropic carbon/epoxy	
In-plane Young's modulus, E_i and E_o	50 GPa
Transverse shear modulus, G_i and G_o	3.80 GPa
Thickness, t_i and t_o	1.0 mm
Adhesive shear modulus, G_a	0.91 GPa
Bond overlap length, $2c$	12.7 mm

Note that while results generated by the UBT and Volkersen solutions are not rigorously applicable to cases of varying bondline thickness (since they do not account for the bond thickness variation during their derivation) these solutions are in closed form and, therefore, testing if they produce useful results is of practical interest.

Five example calculations are presented, starting with a joint having uniform bondline thickness, and investigating joints with increasing severity of thickness variation (decreasing bond thickness at $x = -c$). The variation of bondline thickness $t_a(x)$ is represented using either a quadratic or an exponential function (see Figure 2):

$$t_a = a_o + a_1 x + a_2 x^2, \tag{23}$$

$$t_a = a_o + a_1 e^{a_2 x}. \tag{24}$$

For all calculations, the joint parameters listed in Table 1 were used. These correspond to the quasi-isotropic carbon/epoxy adherend and adhesive properties used in calculations by Tsai *et al*. [7].

Case 1: Uniform Bondline Thickness

The first example calculation, Case 1, is a joint having uniform bondline thickness of 0.152 mm. Results of the VBT solution are compared with the UBT, Volkersen, and FEA predictions in Figure 6. Note that results are normalized with respect to average shear stress, which is the applied load divided by the overlap length,

$$\tau_{ave} = \frac{N_x}{2c}. \tag{25}$$

The VBT and UBT solutions are identical for uniform thickness, as expected. The FEA results were obtained from nodes along the adhesive midplane.

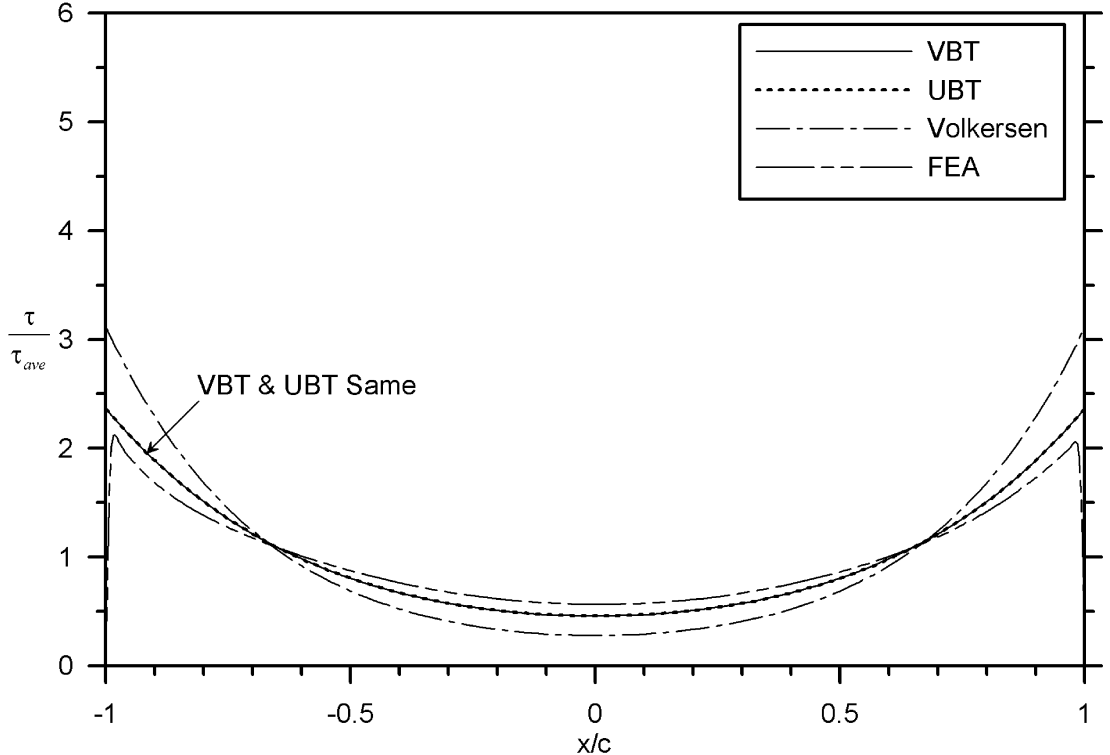

FIGURE 6 Shear stress for Case 1: Uniform $t_a = 0.152\,\text{mm}$.

Cases 2 and 3: Quadratic Thickness Variation

A quadratic polynomial, Equation (23), is used to represent the variation of bondline thickness. Two cases of increasing severity of bond thickness variation were investigated. These cases analyze the effect of one end ($x = -c$) getting thinner while the other end ($x = c$) remains the original 0.152 mm (per Case 1). At $x = -c$, the bondline thickness is 0.051 mm for Case 2, and 0.025 mm for Case 3. In both cases, the slope, dt_a/dx, at $x = c$ was zero.

The VBT, UBT, Volkersen, and FEA predictions are compared with each other in Figures 7 and 8 for Cases 2 and 3, respectively. In both of these cases, the shear stress at $x = -c$ is predicted to increase significantly, in comparison with the uniform thickness case.

Cases 4 and 5: Exponential Thickness Variation

The 0.051 to 0.152 mm thickness variation (per quadratic Case 2) is investigated further by assuming exponential functions to represent the bondline thickness. The thickness function fitting parameters were chosen for these two cases to result in increasingly larger slope dt_a/dx at $x = -c$. In Case 2 (quadratic), the slope is 0.016. In Cases 4 and 5, the slopes are 0.032 and 0.064, respectively.

The results for these cases are similar to the results plotted in Figure 7 for Case 2, and therefore are not plotted. However, the value of peak shear stress at $x = -c$ was found to increase slightly with increasing initial slope. These results are summarized, together with the results from all cases, in Table 2.

DISCUSSION

While the results presented in Table 2 and in Figures 6 to 8 are specific to the joint parameters listed in Table 1, they illustrate some general features. As expected, the maximum value of shear stress in the adhesive increases with severity of thickness imperfection. A range of maximum shear stress was predicted by the four methods for each case analyzed. The FEA is considered to be most accurate since no simplifying assumptions (*e.g.*, shear lag) were made. Except in the case of the uniform joint, the VBT and UBT predictions tended to predict values of maximum shear stress that are lower than the FEA results. In all cases, the Volkersen predictions were much higher (over 44%) than the FEA results. The VBT predictions were the closest in value, relative to the FEA results, with increasing "error" as the bondline got thinner. These observations indicate that the VBT and

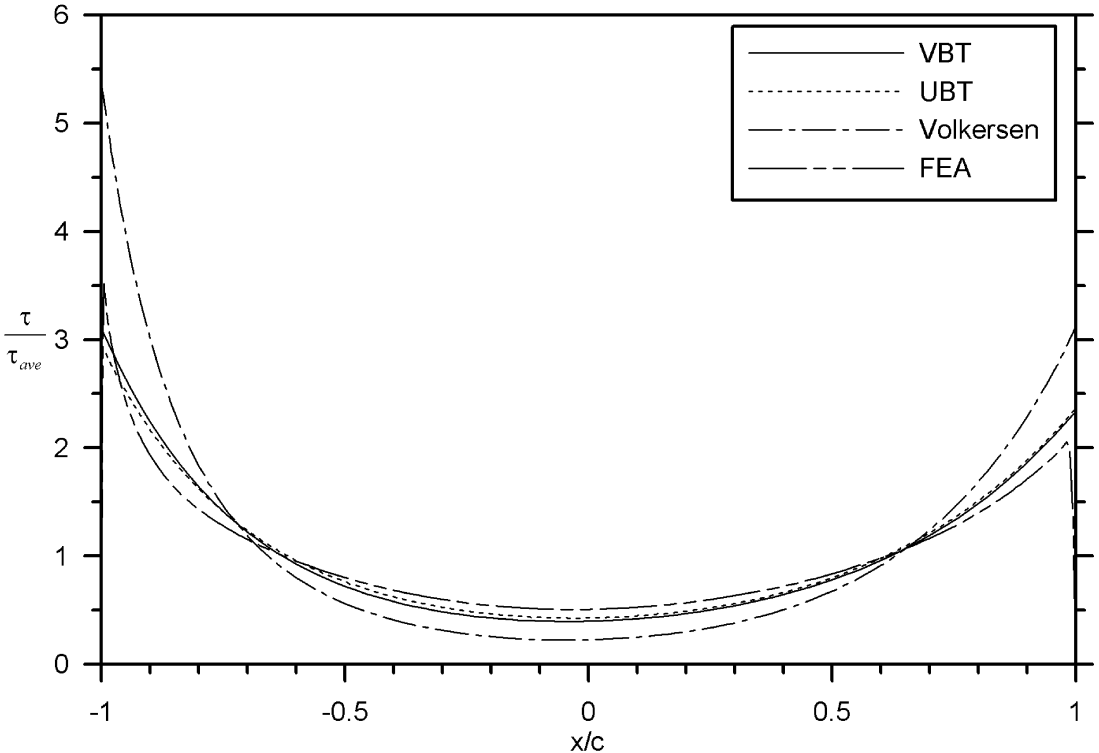

FIGURE 7 Shear stress for Case 2: Quadratic t_a variation from 0.051 to 0.152 mm.

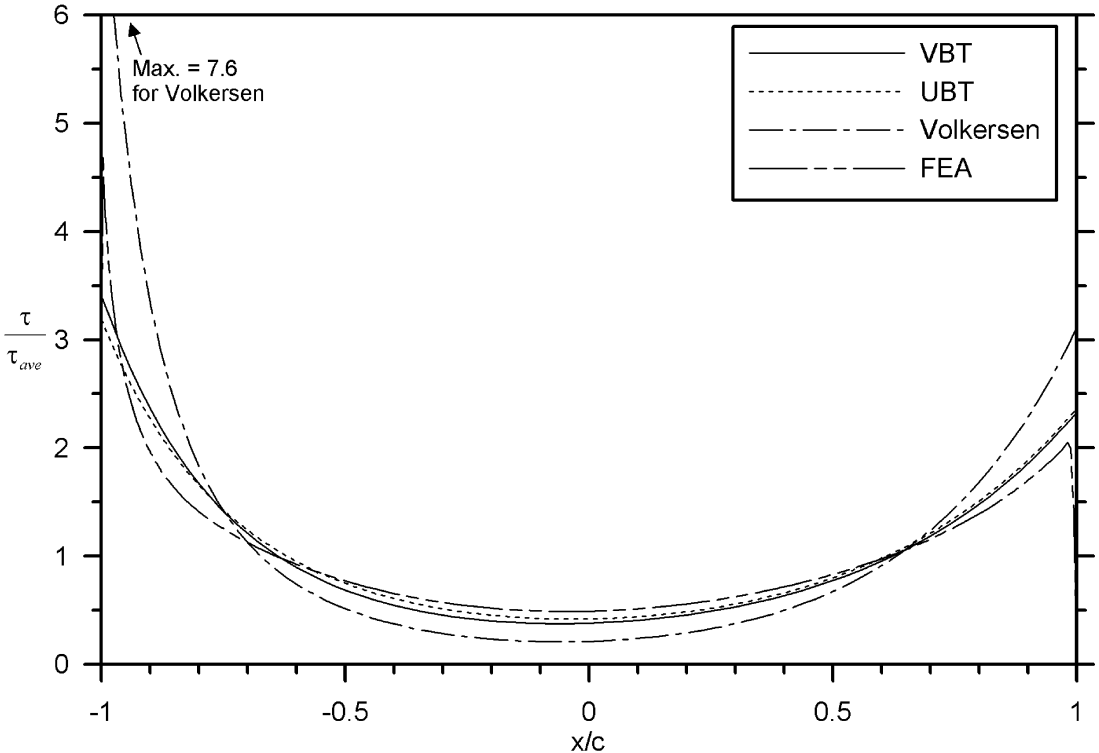

FIGURE 8 Shear stress for Case 3: Quadratic t_a variation from 0.025 to 0.152 mm.

TABLE 2 Comparison of VBT, UBT, and Volkersen Predictions with FEA Results

Case no.	$t_a(-c)$ (mm)	$t_a(c)$ (mm)	$\frac{dt_a}{dx}(-c)$	t_a Profile	τ_{max}/τ_{ave} at $x=-c$ (% difference from FEA)			
					FEA	VBT	UBT	Volkersen
1	0.152	0.152	0	Unif.	2.16	2.36 (+9.3%)	2.37 (+9.7%)	3.12 (+44%)
2	0.051	0.152	0.016	Quad.	3.52	3.1 (−12%)	2.95 (−16%)	5.37 (+53%)
3	0.025	0.152	0.020	Quad	4.71	3.40 (−28%)	3.19 (−32%)	7.60 (+61%)
4	0.051	0.152	0.032	Expon.	3.56	3.18 (−11%)	2.95 (−17%)	5.37 (+51%)
5	0.051	0.152	0.064	Expon.	3.60	3.29 (−8.6%)	2.95 (−18%)	5.37 (+49%)

UBT solutions, which account for adherend transverse shear deformation, tend to provide an overcorrection to the shear stress prediction.

For these case examples investigated, the UBT and VBT predictions were quite close to each other, within 11%, with the tendency to diverge for cases with higher slopes dt_a/dx at $x=-c$. Observe in the governing Equation (13) that when dt_a/dx approaches zero, the VBT governing equation approaches that of the UBT. Note in Table 2 that the UBT and Volkersen solutions for cases 2, 4, and 5 each predict the same peak shear stress for $t_a(-c)=0.051\,\text{mm}$ because they are insensitive to the effect of slope. The reason for this insensitivity is that they are mathematically incorrect for the case of varying bondline, *i.e.*, their derivations did not retain the first derivatives of t_a and T_o. Another point to note is that the UBT and Volkersen solutions, when applied to joints with varying bondline thickness, produce shear stress profiles that do not equilibrate with the applied load, *i.e.*, the integral of the shear stress from $x=-c$ to $+c$ does not equal the average shear stress $N_x/2c$. Despite these points, in joints having practical geometry, the magnitude of possible slope dt_a/dx will be relatively small, and as Figures 7 and 8 show, the UBT formula, Equation (20), can be used to obtain a quick solution. As mentioned before, the Volkersen predictions were always greater than the FEA results. Therefore, both the UBT and Volkersen solutions can be considered together as lower and upper bounding predictions, respectively.

Peel stress, while not predicted by the VBT solution, can be calculated using FEA. In Figure 9, plots of peel stress for Cases 1 and 2 show that the peak peel stress at $x=-c$ is much higher for the varying thickness Case 2 than for the uniform thickness Case 1. Towards $x=c$, the FEA results for the two cases are identical due to the joint

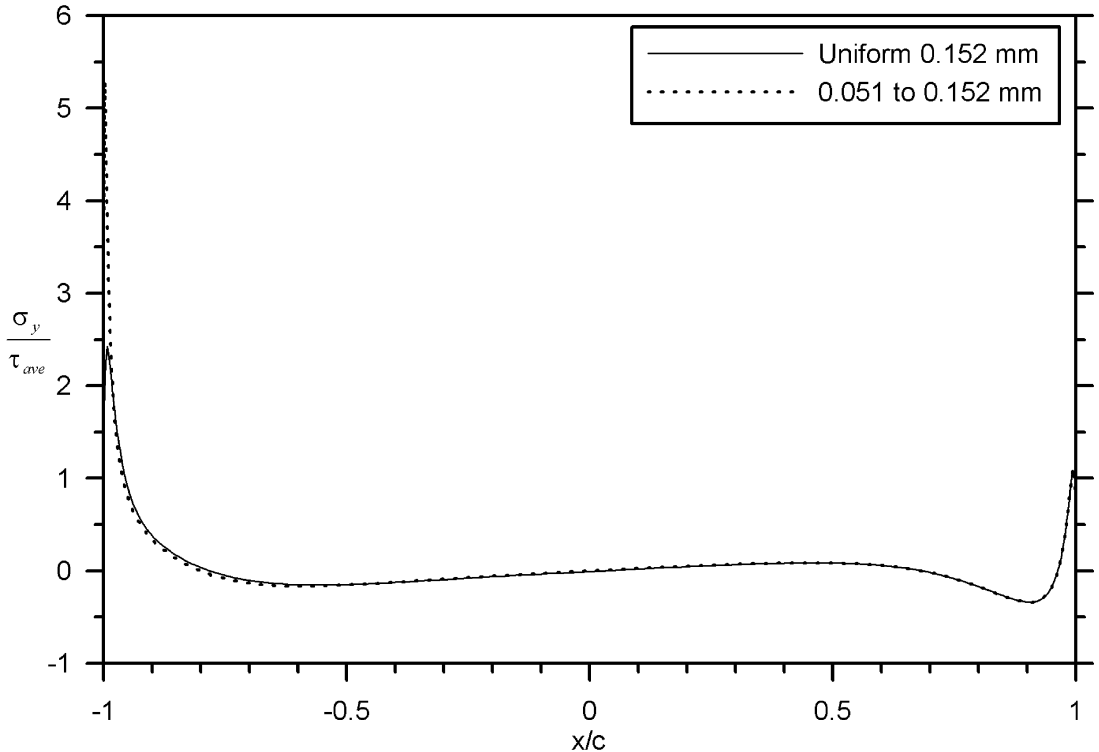

FIGURE 9 FEA Predicted Peel Stress for Cases 1 and 2.

geometry being identical in that region. The significantly higher peel stress at $x = -c$ for Case 2 is a thickness-based effect, rather than a thickness gradient dt_a/dx effect, since gradients of shear stress are generally steeper for thinner (uniform) bondlines; gradients in shear stress are directly related to peel stress. A truly accurate calculation of failure in a bonded joint needs to account for both the peel stress and shear stress. However, since linearly elastic calculations not accounting for adhesive ductility are generally much more conservative than when plasticity is accounted for [14], analysis based only on shear stress can be considered as adequate for design calculations.

A final note on convergence of the Finite Difference calculations is needed. All results presented were computed for a node spacing of 0.127 mm, with a stopping condition of 10^{-5}. This stopping condition applies to the difference in values of T_o calculated between iteration steps. If values are found greater than 10^{-5} anywhere in the solution domain, another iteration is executed. Several thousand iterations are typically needed to achieve a converged solution. Convergence studies show that this combination of stopping condition and node spacing produces results that are less than 1% lower than results produced when an order of magnitude smaller node spacing is used. Additionally, relaxing the stopping condition to 10^{-3} has been found to result in less than 0.5% change in the predicted peak shear stress. Since the VBT predictions are numerical-based, this type of convergence check of the solutions must always be done.

DESIGNING FOR BONDLINE THICKNESS VARIATION

In the manufacture of joints, it is very difficult to achieve uniform bondline thickness geometry, particularly for large-scale bonded assemblies. Therefore, it must be assumed that thickness imperfections will exist, the degree of which can be ascertained on the manufacturing floor. Alternatively, for quality control purposes, it is desirable for a range of bondline thickness imperfection acceptance limits to be established even before parts are produced.

Using the VBT solution derived herein, joints can be designed to account for thickness imperfections. Of interest is: how much of an increase in shear stress occurs for a joint with thinning bondline relative to a joint having uniform bondline (assumed to be designed geometry)? To answer this question, a series of joints were analyzed, starting with a uniform thickness joint, and progressively decreasing the bondline thickness $t_a(-c)$ at $x = -c$ (see Figure 2). In each joint, the bondline thickness $t_a(c)$ remained the same at $x = c$. As summarized in

Table 2, higher peak shear stress values were predicted for joints with thinning bondline. These higher stresses were compared with the peak stress for the uniform thickness case and are plotted using the functional form derived from the UBT solution, Equation (20):

$$\frac{\tau_1}{\tau_{unif}} \cdot \frac{\alpha_1}{\alpha_{unif}} = f \cdot \left(\frac{t_1}{t_{unif}}\right)^{-\frac{1}{2}} \tag{26}$$

In Equation (26) τ_1 is the peak shear stress in the imperfect joint at $x = -c$, while τ_{unif} is the peak shear stress for the corresponding uniform joint (design-intended geometry). α_1 and α_{unif} are the nondimensional transverse shear stiffness geometric/material parameters given by Equation (15) corresponding to thickness $t_1 = t_a(-c)$ and $t_{unif} = t_a(c)$, respectively. f is a nondimensional nonlinear parameter that is a function of all the joint material and geometric parameters.

The effect of each parameter on f in Equation (26) was studied by varying each parameter individually over a wide range of values. By this process, a bounding set of extreme parameter values were determined that gives an upper and lower bound of the function f. Table 3 lists the parameters that influence f together with upper and lower bounding values. The column of up and down arrows indicates in what manner increasing values of the parameter cause changes in f. For example, increasing values of bond overlap length 2c were found to decrease values of f. An exception was found for the adherend thickness producing upper bound values of f. While thicker adherends resulted in a monotonic decrease in f, a unique value of t_i and t_o exists for a given choice of other parameter values, such that f is maximum.

TABLE 3 Extreme Parameter Values Giving Upper and Lower Bounds for f

Parameter	Effect of increasing parameter on f	Upper bound	Lower bound
Adherends			
In-plane Young's modulus, E_i and E_o	↑	207 GPa	6.98 GPa
Transverse shear modulus, G_i and G_o	↑	80.3 GPa	3.86 GPa
Thickness, t_i and t_o	↓	0.508 mm*	12.7 mm
Adhesive			
Shear modulus, G_a	↓	0.698 GPa	2.10 GPa
Uniform joint thickness, t_{unif}	↑	1.27 mm	0.127 mm
Bond overlap length, $2c$	↓	10.2 mm	102 mm

*Decreasing t_i and t_o did not monotonically give higher f. Value used is unique for given choice of other parameters.

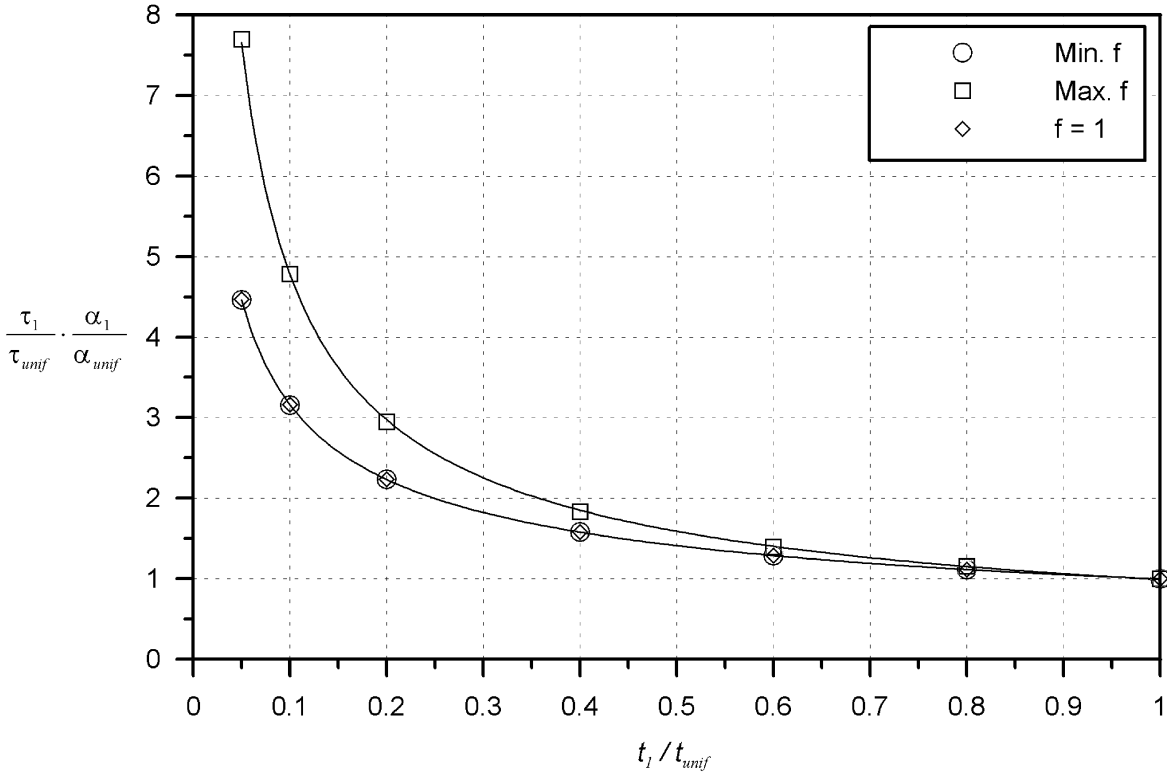

FIGURE 10 Peak shear stress for joints with varying bondline thickness relative to peak shear stress in uniform joints.

The parameters listed in Table 3 were used to compute ratios of predicted peak shear stress in imperfect joints compared with peak shear stress in joints having uniform bondline. This ratio, following the form of Equation (26), are plotted in Figure 10 as a function of thickness imperfection, t_1/t_{unif}. When $t_1/t_{unif} = 1$, the joint has uniform thickness and therefore there is no increase in peak shear stress. As the joint thins at $x = -c$, higher peak shear stresses are predicted. Values chosen in Table 3 reflect a realistic range of parameter values. For example, in the upper bound column a high adherend Young's modulus is desired, so steel was chosen as the material, giving a value of 207 GPa. Also plotted in Figure 10 is the case for f assumed to have a value of unity ($f = 1$). Comparison with f computed from lower bounding parameter values indicates the $f = 1$ case to be a minimum.

Figure 10 has been presented in a manner facilitating design calculation of stresses in bonded joints having localized thinning. For a given range of expected thickness imperfection, t_1/t_{unif}, upper and lower bounding values of $\tau_1\alpha_1/\tau_{unif}\alpha_{unif}$ can be read off from the vertical axis of Figure 10. These values effectively act as "stress concentration factors" that account for thickness imperfection severity. For most practical joints, the bond overlap length $2c$ will be relatively long such that the shear stress peaks at the overlap ends do not influence each other. In these cases, Figure 10 can be used to evaluate joints having thinning at both overlap ends. For example, the joint shown in Figure 1 varies from 0.15 mm at the center to 0.04 mm at the ends. The intended thickness for this joint was 0.15 mm, so a thickness imperfection of $t_1/t_{unif} = 0.27$ exists. Using Figure 8, $\tau_1\alpha_1/\tau_{unif}\alpha_{unif}$ ranges between 1.9 to 2.4.

CONCLUSIONS

Relative to a joint with uniform bondline thickness, the adhesive shear stress dramatically increases when the adhesive bondline thins at the joint ends, *i.e.*, at $x = \pm c$. To predict this increase, a shear lag-based analysis was developed that predicts the adhesive shear stress and accounts for varying bondline thickness. In the derived differential equation found to govern this problem, varying bondline thickness appears as a term containing the first derivative of bondline thickness, dt_a/dx. Solution to this governing equation, referred to as the VBT solution, was found to be accurate relative to FEA results for cases of moderate bondline thinning. The VBT solution tended to underpredict the FEA predictions by up to 28% for the cases studied.

The capabilities of a closed-form uniform bondline thickness (UBT) solution, and the classical Volkersen solution were investigated. The UBT solution, while close to the more accurate VBT solution, tended to underpredict the FEA results even more. The UBT and VBT solutions matched well for cases of moderate thickness slope, dt_a/dx. Based on the case study results, a slope of $dt_a/dx < 0.064$ resulted in less than 20% underprediction (relative to FEA) by the UBT solution, and less than 9% underprediction by the VBT solution. The UBT solution, since it is in closed form, is desirable for quick solutions and can be used with acceptable accuracy for cases of moderate thickness slope.

Since the Volkersen solution greatly overpredicted the FEA results (up to 61%) and the UBT consistently underpredicts, these two analysis can be used to obtain, in closed-form, upper and lower bounding predictions of the increase in adhesive shear stress due to thickness imperfection. Alternatively, a "stress concentration factor" chart (Figure 10) was presented that summarized a series of VBT solutions that were created using parameter sets such that extreme ranges in adhesive stress increase were predicted. This chart would give more tightly-bounding upper and lower bound predictions than the UBT and Volkersen calculations, and can be used to assess quickly the effects of thickness imperfection severity on the peak adhesive shear stress.

REFERENCES

[1] Volkersen, O., *Luftfahrtforschung*, **15**, 41–47 (1938).
[2] Hart-Smith, L. J., NASA-Langley Contract Report, NASA-CR-112235 (1973).
[3] Hart-Smith, L. J., *Joining of Composite Materials, ASTM STP 749*, K. T. Kedward, Ed. ASTM, 3–31 (1981).
[4] Goland, M. and Reissner, E., *J. Applied Mechanics*, **11**, A17–A27 (1944).
[5] Ojalvo, I. U. and Eidinoff, H. L., *AIAA J.*, **16**(3), 204–211 (1978).
[6] Oplinger, D. W., *Int. J. Solids Structures*, **31**(18), 2565–2587 (1994).
[7] Tsai, M. Y., Oplinger, D. W. and Morton, J., *Int. J. Solids Structures*, **35**(12), 1163–1185 (1998).
[8] Gleich, D. M., van Tooren, M. J. L., and Beukers, A., *Proc. 32nd Intl. SAMPE Technical Conference*, November 5–9, (2000), pp. 567–579.
[9] Li, G., Lee-Sullivan, P. and Thring, R. W., *Composite Structures*, **46**, 395–403 (1999).
[10] Kline, R. A., *Proc. Int. Symposium on Adhesive Joints: Formation, Characteristics, and Testing*, September 12–17, (1984), pp. 587–610.
[11] Wang, C. H. and Rose, L. R. F., *Int. J. Adhesion and Adhesives*, **20**, 145–154 (2000).
[12] Rispler, A. R., Tong, L., Steven, G. P. and Wisnom, M. R., *Int. J. Adhesion and Adhesives*, **20**, 221–231 (2000).
[13] Hibbitt, Karlsson and Sorensen, *ABAQUS/Standard Version 6.2 User's Manual* (2001).
[14] Lee, J. and Kim, H., *Proc. American Society for Composites 17th Technical Conference*, West Lafayette, IN, October 21–23 (2002).